Intramolecular Coupling of η^2-Iminoacyl and η^2-Acyl Functions at Group 4 and Group 5 Metal Centers; Structure and Spectroscopic Properties of the Resulting Enamidolate and Enediamide Complexes

Linda R. Chamberlain, Loren D. Durfee, Phillip E. Fanwick, Lisa M. Kobriger, Stanley L. Latesky, Anne K. McMullen, Bryan D. Steffey, Ian P. Rothwell,*[1] Kirsten Folting, and John C. Huffman

Contribution from the Department of Chemistry, Purdue University, West Lafayette, Indiana 47907, and Molecular Structure Center, Indiana University, Bloomington, Indiana 47405. *Received December 9, 1986*

Abstract: A series of group 4 and group 5 metal aryloxide compounds containing enamidolate or enediamide ligation have been prepared by the intramolecular coupling of η^2-acyl and η^2-iminoacyl functional groups. For the group 4 metals reaction of the mono-iminoacyl's $(ArO)_2M(\eta^2\text{-}R'NCR)(R)$ (M = Ti, Ar = 2,6-diisopropylphenyl, R = CH_2Ph; M = Zr, Ar = 2,6-di-*tert*-butylphenyl, R = CH_2Ph) with carbon monoxide (700-1000 psi) leads directly to the corresponding enamidolate (I) with no evidence for the presumed intermediate mixed acyl, iminoacyl compound. However, the isolable bis η^2-iminoacyl compounds $(ArO)_2M(\eta^2\text{-}R'NCR)_2$ (M = Ti, Zr, Hf; ArO = 2,6-diisopropyl-, 2,6-diphenyl-, and 2,6-di-*tert*-butylphenyl; R = CH_3, CH_2Ph) only undergo intramolecular coupling to the corresponding enediamide derivatives (II) on thermolysis in hydrocarbon solvents. In contrast, attempts to prepare a bis η^2-iminoacyl derivative of $Ti(OAr\text{-}2,6\text{-}Ph_2)_2(\eta^2\text{-}PhNCCH_2SiMe_3)(CH_2SiMe_3)$ (OAr-2,6Ph_2 = 2,6-diphenylphenoxide) by addition of PhNC led only to the isolation of a tris-inserted, coupled complex $Ti(OAr\text{-}2,6Ph_2)_2[PhNCR{=}C(CR{=}NPh)NPh]$ (III) (R = CH_2SiMe_3) containing an enediamide chelate with an imine substituent on the carbon backbone. The tantalum bis η^2-iminoacyl $Ta(OAr\text{-}2,6Me_2)_3(\eta^2\text{-}xyNCCH_2Ph)_2$ undergoes the clean formation of the enediamide $Ta(OAr\text{-}2,6Me_2)_3[xyNC(CH_2Ph){=}C(CH_2Ph)Nxy]$ (IV) on thermolysis at 110 °C. Single-crystal X-ray diffraction studies on six compounds of types I, II, III, and IV have been carried out. In the enamidolate compounds $Ti(OAr\text{-}2,6Pr^i_2)_2[OC(CH_2Ph){=}C(CH_2Ph)NBu^t]$ (Ia) and $Zr(OAr\text{-}2,6Bu^t_2)_2[OC(CH_2Ph){=}C(CH_2Ph)Nxy]$ (Ib) both molecules were found to contain a pseudotetrahedral geometry about the metal. The 5-membered metallacycle formed by the enamidolate chelate ring was found to be nonplanar with the metal atom lying out of the plane of the OC=CN backbone. Despite fold angles of 51.1° and 50.0°, respectively, solution NMR spectra indicated that inversion of the bent metallacycle was facile. For the related group 4 metal enediamide compounds $Ti(OAr\text{-}2,6Pr^i_2)_2[xyNC(CH_2Ph){=}C(CH_2Ph)NBu^t]$ (IIc), $Zr(OAr\text{-}2,6Bu^t_2)_2[xyNC(CH_3){=}C(CH_3)Nxy]$ (IId) and $Ti(OAr\text{-}2,6Ph_2)_2[PhNC(R){=}C(CR{=}NPh)NPh]$ (III) (R = CH_2SiMe_3) a similar, nonplanar geometry for the chelate ring is observed. However, in this case a significant barrier (12-17 kcal mol^{-1}) to inversion of the bent metallacycle ring is indicated by analysis of the temperature dependence of the ^1H NMR spectra of compounds of type II and III. In contrast the compound $Ta(OAr\text{-}2,6Me_2)_3[xyNC(CH_2Ph){=}C(CH_2Ph)Nxy]$ (IV) was found to contain an essentially planar metallacycle, the two nitrogen atoms of the enediamide chelate occupying one axial and one equatorial position about the 5-coordinate, trigonal-bipyramidal, metal atom. Structural parameters for all of the coupled products obtained in this study are totally consistent with them being viewed as containing enamidolate and enediamide ligands bound to Ti^{IV}, Zr^{IV}, and Ta^V, d°-metal centers with little support for an alternate situation involving 1-oxa-4-aza-1,3-butadiene or 1,4-diaza-1,3-butadiene ligand resonance forms. The summary of the crystal data is as follows: for $Ti(OAr\text{-}2,6Pr^i_2)_2[OC(CH_2Ph){=}C(CH_2Ph)NBu^t]$ (Ia) at -154 °C, a = 19.877 (8) Å, b = 12.065 (4) Å, c = 16.939 (7) Å, β = 102.79 (2)°, Z = 4, d_{calcd} = 1.167 g cm^{-3} in space group $P2_1/a$; for $Zr(OAr\text{-}2,6Bu^t_2)_2[OC(CH_2Ph){=}C(CH_2Ph)Nxy]$ (Ib) at -160 °C, a = 20.445 (9) Å, b = 11.750 (4) Å, c = 10.059 (3) Å, α = 93.63 (1)°, β = 88.56 (1)°, γ = 88.73 (1)°, Z = 2, d_{calcd} = 1.173 g cm^{-3} in space group $P\bar{1}$; for $Ti(OAr\text{-}2,6Pr^i_2)_2[xyNC(CH_2Ph){=}C(CH_2Ph)NBu^t]$ (IIc) at 22 °C, a = 11.751 (4) Å, b = 15.113 (4) Å, c = 26.282 (6) Å, β = 92.13 (2)°, Z = 4, d_{calcd} = 1.138 g cm^{-3} in space group $P2_1/c$; for $Zr(OAr\text{-}2,6Bu^t_2)_2[xyNC(CH_3){=}C(CH_3)Nxy]$ (IId) at -161 °C, a = 17.657 (6) Å, b = 14.820 (5) Å, c = 16.510 (3) Å, β = 95.60 (5)°, Z = 4, d_{calcd} = 1.230 g cm^{-3} in space group $P2_1/n$; for $Ti(OAr\text{-}2,6Ph_2)_2[PhNC(R){=}C(CR{=}NPh)NPh]\cdot{}^1/_2C_6H_{14}$ (R = CH_2SiMe_3) (III) at -155 °C, a = 30.390 (15) Å, b = 13.355 (6) Å, c = 15.232 (7) Å, β = 105.04 (2)° Z = 4, d_{calcd} = 1.185 g cm^{-3} in space group $P2_1/a$; for $Ta(OAr\text{-}2,6Me_2)_3[xyNC(CH_2Ph){=}C(CH_2Ph)Nxy]$ (IV) at -152 °C, a = 18.869 (b) Å, b = 13.006 (5) Å, c = 21.971 (8) Å, β = 119.46 (6)°, Z = 4, d_{calcd} = 1.399 g cm^{-3} in space group $P2_1/c$.

The reactivity of high valent early d-block, lanthanide and actinide metal alkyl and related hydride compounds toward carbon monoxide has received considerable study.[2-6] A particularly interesting reactivity that has been demonstrated is the ability of the generated metal acyl or formyl function to undergo carbon-carbon bond-forming reactions. Besides both the intra- and intermolecular coupling to produce cis and trans enediolate ligands,[7,8] further reaction with CO or organic isocyanides has been observed as well.[9,10] The possible relevance of these C-C bond-forming reactions to the catalytic reductive coupling of CO (Fischer-Tropsch) has been widely discussed.[11] The intramolecular coupling of acyl groups at later transition metal centers to produce α-diketones has also been studied.[12] Other somewhat related processes are the reductive coupling of coordinated carbonyl[13] and organic isocyanide ligands either at mono- or dimetal centers.[14]

During our studies of the early d-block metal chemistry associated with aryloxide ligation we have examined the reactivity of

* Address correspondence to this author at Purdue University.

(1) (a) Camille and Henry Dreyfus Teacher-Scholar, 1985-1990. (b) Fellow of the Alfred P. Sloan Foundation, 1986-1990.

(2) (a) Wolczanski, P. T.; Bercaw, J. E. *Acc. Chem. Res.* **1980**, *13*, 121. (b) Erker, G. *Acc. Chem. Res.* **1984**, *17*, 103.

(3) Curtis, M. D.; Shiu, K. b.; Butler, W. M. *J. Am. Chem. Soc.* **1986**, *108*, 1550 and references therein.

(4) (a) Evans, W. J. *Adv. Organomet. Chem.* **1985**, *24*, 131. (b) Evans, W. J.; Wayda, A. L.; Hunter, W. E.; Atwood, J. L. *J. Chem. Soc., Chem. Commun.* **1981**, 706.

(5) (a) Marks, T. J.; Day, V. W. In *Fundamental and Technological Aspects of Organo-f-Element Chemistry*; Marks, T. J., Fragala, I. L., Eds.; Dordrecht: Holland, 1986. (b) Moloy, K. G.; Marks, T. J. *J. Am. Chem. Soc.* **1981**, *103*, 3576.

(6) Theoretical Studies of the bonding of η^2-acyl groups have been carried out, see: Tatsumi, K.; Nakamura, A.; Hoffmann, R. *Organometallics* **1985**, *4*, 404.

0002-7863/87/1509-6068$01.50/0

Scheme I

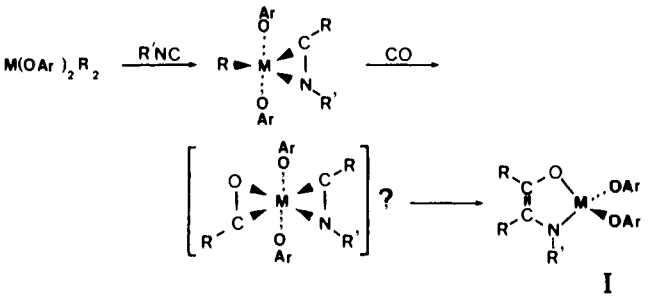

(Ia): M = Ti; OAr = OAr-2,6Pr$^i_2$; R = CH_2Ph; R' = Bu^t

(Ib): M = Zr; OAr = OAr-2,6Bu$^t_2$; R = CH_2Ph; R' = xy

a series of mixed alkyl, aryloxide compounds toward CO and the isoelectronic organic isocyanide molecule. This has allowed us to isolate and study in detail a series of compounds containing a number of η^2-iminoacyl functions.[15] Furthermore we have demonstrated that intramolecular coupling of iminoacyl groups to produce enediamido ligands can take place, as well as the related coupling of iminoacyl and acyl groups.[16] We report here in detail the synthesis of a number of enamidolate and enediamido complexes using this synthetic method and also report in detail on the coordination properties of the resulting metallacycles, an area that has received recent theoretical interest.[17] In a subsequent paper we report a kinetic investigation of these carbon–carbon bond-forming processes.[18]

Results and Discussion

Synthesis of Compounds. Enamidolate Compounds. The mixed alkyl, iminoacyl complexes Ti(OAr-2,6Pr$^i_2$)$_2$(η^2-Bu^{t}NCCH$_2$Ph)(CH$_2$Ph) and Zr(OAr-2,6Bu$^t_2$)$_2$(η^2-xyNCCH$_2$Ph)(CH$_2$Ph) (OAr-2,6R$_2$ = 2,6-dialkylphenoxide) will readily insert another equivalent of organic isocyanide into the M–R bond to form stable bis iminoacyl derivatives.[15] Carbonylation of the monoalkyl compounds was attempted in order to try and isolate the related mixed acyl, iminoacyl derivatives for study. Both substrates were found to be stable in solution for days under 1 atm of CO. However, under more forcing conditions (200–1000 psi) both compounds absorbed 1 equiv of CO in hydrocarbon solvents to generate the corresponding enamidolate complexes Ia and Ib in excellent yields (Scheme I). Analysis (^{1}H NMR) of the reaction mixtures after only partial carbonylation indicated the presence in solution of only the monoalkyl substrate and enamidolate product I. No evidence for the presumed intermediate mixed acyl, iminoacyl (Scheme I) was obtained. The migratory insertion of CO into a metal–carbon bond of the metallocene dialkyls Cp$_2$MR$_2$ (M = Ti, Zr, Hf) has been shown to be readily reversed.[19] Hence the lack of detectable amounts of this intermediate may reflect either its instability with respect to deinsertion of CO under ambient pressures or else imply an immediate, facile coupling process taking place upon its formation.

Scheme II

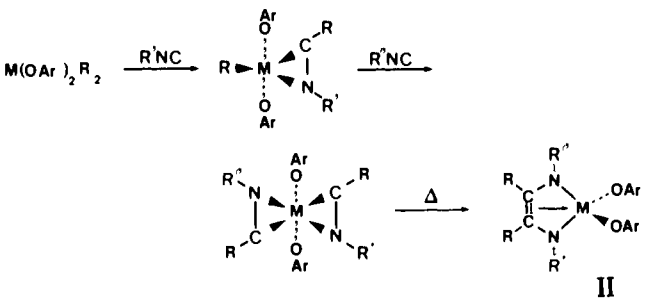

	M	OAr	R	R'	R''
(IIa)	Ti	OAr-2,6Pr$^i_2$	CH_2Ph	xy	xy
(IIb)	Ti	OAr-2,6Pr$^i_2$	CH_2Ph	Ph	Bu^t
(IIc)	Ti	OAr-2,6Pr$^i_2$	CH_2Ph	xy	Bu^t
(IId)	Zr	OAr-2,6Bu^t	CH_3	xy	xy
(IIe)	Zr	OAr-2,6Bu$^t_2$	CH_2Ph	Ph	Ph
(IIf)	Zr	OAr-2,6Bu$^t_2$	CH_3	Ph	Ph
(IIg)	IIf	OAr-2,6Bu$^t_2$	CH_3	Ph	Ph

Enediamido Compounds. We have previously shown that the migratory insertion of organic isocyanides into both metal alkyl bonds of compounds of stoichiometry M(OAr)$_2$(R)$_2$ (M = Ti, Zr, Hf) leads to the corresponding bis η^2-iminoacyl derivatives in excellent yield.[15] These compounds undergo intramolecular coupling of the two iminoacyl groups on mild thermolysis in hydrocarbon solvents to generate the enediamido compounds II in essentially quantitative yield as judged by ^{1}H NMR (Scheme II). For zirconium we have confirmed this reactivity for a large number of different nitrogen substituents and carried out a kinetic study that will be reported in detail in a later paper.[18] However, for the purpose of this study we have focused on the compounds shown in Scheme II.

The use of the mono iminoacyl complex Ti(OAr-Pr$^i_2$)$_2$(η^2-Bu^{t}NCCH$_2$Ph)(CH$_2$Ph)[15] has allowed us to isolate asymmetrically substituted enediamide ligands. Hence the addition of 1 equiv of phenyl isocyanide (PhNC) leads to the formation of the coupled product IIc in essentially quantitative yields (Scheme II). The intermediate, bis iminoacyl complex was observed spectroscopically but was not isolated due to the rapid rate at which intramolecular coupling occurs. However, use of the more bulk 2,6-dimethylphenyl isocyanide (xyNC) slows down the coupling process and allows the isolation of the intermediate prior to coupling on thermolysis.

In contrast to this behavior, the bright yellow mono η^2-iminoacyl Ti(OAr-2,6Ph$_2$)$_2$(η^2-PhNCCH$_2$SiMe$_3$)(CH$_2$SiMe$_3$)[15] will react rapidly with two more equivalents of phenyl isocyanide in benzene to give the deep red "tris-insertion" compound III as shown in Scheme III. When only 1 equiv of PhNC is added an approximately 50/50 mixture of III and the initial substrate is formed with no evidence for significant quantities of a presumed intermediate bis-insertion compound. Compound III contains an enediamide chelate similar to that found in compound II except that now an extra molecule of isocyanide has been incorporated into the chelate backbone. This we believe comes about via a double insertion of two PhNC molecules into one of the Ti–CH$_2$SiMe$_2$

(7) (a) Manriquez, J. M.; D. R.; Sanner, R. D.; Bercaw, J. E. *J. Am. Chem. Soc.* **1978**, *100*, 2716. (b) Erker, G.; Czisch, P.; Schlund, R.; Angermund, K.; Kreuger, C. *Angew. Chem.* **1986**, *98*, 356.

(8) (a) Tatsumi, K.; Nakamura, A.; Hofmann, P.; Hoffmann, R.; Moloy, K. G.; Marks, T. J. *J. Am. Chem. Soc.* **1986**, *108*, 4467. (b) Evans, W. J.; Grate, J. W.; Doedens, R. J. *J. Am. Chem. Soc.* **1985**, *107*, 1671.

(9) (a) Moloy, K. G.; Fagan, P. J.; Manriquez, J. M.; Marks, T. J. *J. Am. Chem. Soc.* **1986**, *108*, 56. (b) Marks, T. J. *Science* **1982**, *217*, 989.

(10) Evans, W. J.; Grate, J. W.; Hughes, L. A.; Zhang, H.; Atwood, J. L. *J. Am. Chem. Soc.* **1985**, *107*, 3728.

(11) *Catalytic activation of Carbon Monoxide*, Ford, P. C., Ed.; American Chemical Society: Washington, DC, 1981; ACS Sym. Series, Vol. 152.

(12) Ozawa, F.; Soyama, H.; Yanaghiara, H.; Aoyama, I.; Takino, H.; Izawa, K.; Yamamoto, T.; Yamamoto, A. *J. Am. Chem. Soc.* **1985**, *107*, 3235 and references therein.

(13) (a) Berry, D. H.; Bercaw, J. E.; Jircitano, A. J.; Mertes, K. B. *J. Am. Chem. Soc.* **1982**, *104*, 4712. (b) Bianconi, P. A.; Williams, I. D.; Engeler, M. P.; Lippard, S. J. *J. Am. Chem. Soc.* **1986**, *108*, 311.

(14) (a) Gianodomenico, C. M.; Lam, C. T.; Lippard, S. J. *J. Am. Chem. Soc.* **1982**, *104*, 1263. (b) Warner, S.; Lippard, S. J. *Organometallics* **1986**, *5*, 1716.

(15) Chamberlain, L. R.; Durfee, L. D.; Fanwick, P. W.; Kobriger, L.; Latesky, S. L.; McMullen, A. K.; Rothwell, I. P.; Folting, K.; Huffmann, J. C.; Streib, W. E. *J. Am. Chem. Soc.*, in press.

(16) (a) McMullen, A. K.; Rothwell, I. P.; Huffman, J. C. *J. Am. Chem. Soc.* **1985**, *107*, 1072. (b) Latesky, S. L.; McMullen, A. K.; Rothwell, I. P.; Huffman, J. C. *Organometallics* **1985**, *48*, 1986. (c) Chamberlain, L. R.; Rothwell, I. P.; Huffman, J. C. *J. Chem. Soc., Chem. Commun.*, in press.

(17) (a) Hoffman, P.; Frede, M.; Stauffert, P.; Lasser, W.; Thewalt, J. *Angew. Chem., Int. Ed. Engl.* **1985**, *24*, 712. (b) Curtis, M. D.; Real, J. *J. Am. Chem. Soc.* **1986**, *108*, 4668.

(18) Durfee, L. D.; McMullen, A. K.; Rothwell, I. P., results to be submitted for publication.

(19) (a) Fachinetti, G.; Fochi, G.; Florianai, C. *J. Chem. Soc., Dalton Trans.* **1977**, 1946. (b) Fachinetti, G.; Floriani, C.; Stoeckli-Evans, H. *J. Chem. Soc., Dalton Trans.* **1977**, 2297.

Scheme III

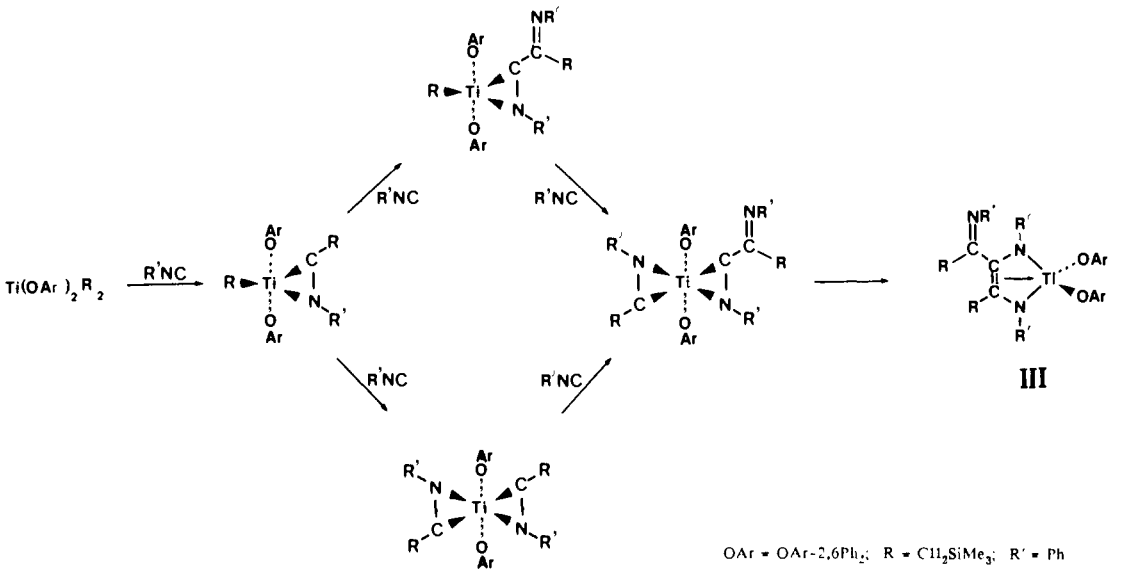

Scheme IV

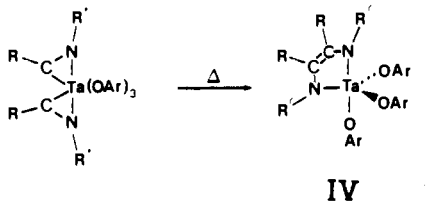

bonds.[20] The resulting intermediate then undergoes intramolecular coupling to the observed final product (Scheme III).

For tantalum we have characterized two general types of bis η^2-iminoacyl derivatives of formulae $Ta(OAr)_2(\eta^2\text{-}R'NCR)_2(R)$ and $Ta(OAr)_3(\eta^2\text{-}R'NCR)_2$.[15] The former compounds exhibit a range of thermal reactivity depending on the substituent R, but no evidence was obtained for the formation of enediamide ligands.[16c] However, the compound $Ta(OAr\text{-}2,6Me_2)_3(\eta^2\text{-}xyNCCH_2Ph)_2$ will undergo intramolecular coupling of the η^2-iminoacyl groups on extended thermolysis (110 °C/48 h) in toluene solution to form the enediamido complex IV as shown (Scheme IV).

Solid-State and Solution Structure. The solid-state structures of six of the coupled products have been determined in order to more fully characterize both their molecular structure as well as the coordination properties of the enamidolate and enediamido ligands.

$Ti(OAr\text{-}2,6Pr^i_2)_2[OC(CH_2Ph)=C(CH_2Ph)NBu^t]$ (Ia) and $Zr(OAr\text{-}2,6\text{-}Bu^t_2)_2[OC(CH_2Ph)=C(CH_2Ph)Nxy]$ (Ib). The molecular structures of Ia and Ib are shown in Figures 1 and 2, respectively. Some important bond distances and angles for both compounds are contained in Table I. Both molecules can be seen to adopt a pseudotetrahedral geometry about the metal atom. The O–M–O angles of 111.1 (1)° and 117.4 (2)° made by the aryloxide ligands are much larger than the 90.1 (1)° and 84.2 (2)° bite of the two enamidolate ligands in Ia and Ib, respectively. The short M–OAr distances and large M–O–Ar angles associated with the aryloxide ligands are typical for these groups bound to high valent early transition metal centers.[21] The M–O distance to the enamidolate ligand in Ia and Ib is consistently longer by approximately 0.05–0.07 Å than the M–O distances to the aryloxide

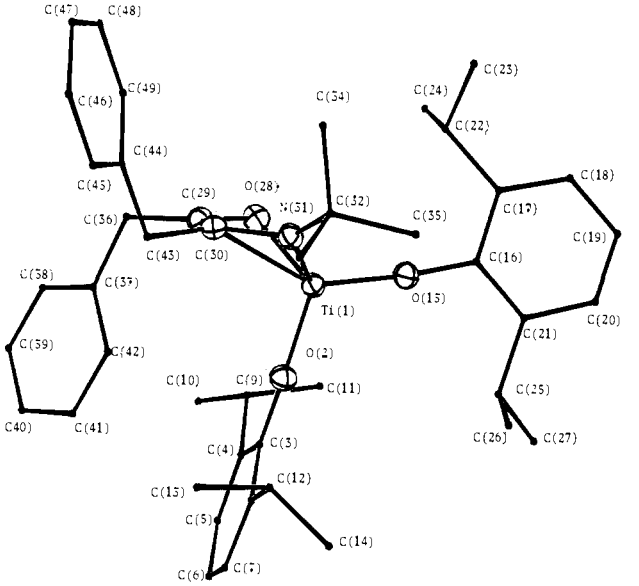

Figure 1. ORTEP view of $Ti(OAr\text{-}2,6Pr^i_2)_2[OC(CH_2Ph)=C(CH_2Ph)\text{-}NBu^t]$ (Ia).

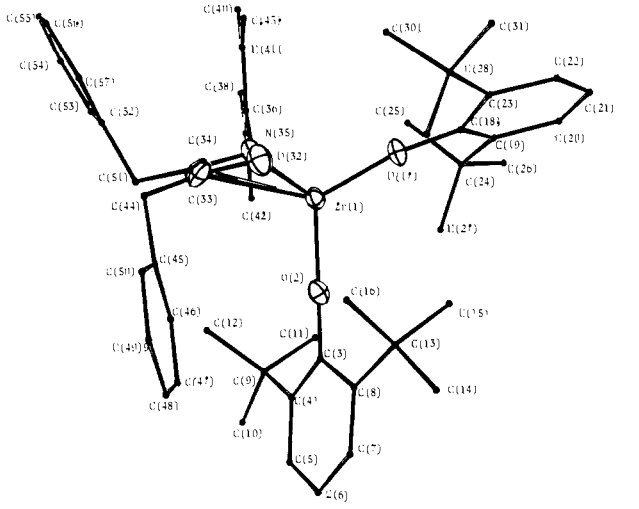

Figure 2. ORTEP view of $Zr(OAr\text{-}2,6Bu^t_2)_2[OC(CH_2Ph)=C(CH_2Ph)\text{-}Nxy]$ (Ib).

(20) Singleton, E.; Oosthuizen, H. E. *Adv. Organomet. Chem.* **1983**, *22*, 209 and references therein.

(21) (a) Coffindaffer, T. W.; Rothwell, I. P.; Folting, K.; Huffman, J. C.; Streib, W. *J. Chem. Soc., Chem. Commun.* **1985**, 1519. (b) Latesky, S. L.; McMullen, A. K.; Niccolai, G. P.; Rothwell, I. P.; Huffman, J. C. *Organometallics* **1985**, *4*, 902. (c) Latesky, S. L.; McMullen, A. K.; Rothwell, I. P.; Huffman, J. C. *J. Am. Chem. Soc.* **1985**, *107*, 5981. (d) Chamberlain, L. R.; Rothwell, I. P.; Huffman, J. C. *J. Chem. Soc., Dalton Trans.*, in press.

Table I. Selected Bond Distances (Å) and Angles (deg) for Ia and Ib

Ia		Ib	
Ti(1)–O(2)	1.814 (3)	Zr(1)–O(2)	1.967 (5)
Ti(1)–O(15)	1.792 (3)	Zr(1)–O(17)	1.929 (5)
Ti(1)–O(28)	1.877 (3)	Zr(1)–O(32)	2.004 (5)
Ti(1)–N(31)	1.893 (3)	Zr(1)–N(35)	2.038 (6)
Ti(1)–C(29)	2.398 (4)	Zr(1)–C(33)	2.549 (8)
Ti(1)–C(30)	2.4929 (4)	Zr(1)–C(34)	2.581 (8)
O(28)–C(29)	1.373 (4)	O(32)–C(33)	1.377 (9)
C(29)–C(30)	1.375 (6)	C(33)–C(34)	1.348 (11)
C(30)–N(31)	1.412 (4)	C(34)–N(35)	1.434 (10)
O(2)–Ti(1)–O(15)	111.1 (1)	O(2)–Zr(1)–O(17)	117.4 (2)
O(2)–Ti(1)–O(28)	115.8 (1)	O(2)–Zr(1)–O(32)	113.7 (2)
O(2)–Ti(1)–N(31)	116.1 (1)	O(2)–Zr(1)–N(35)	120.2 (2)
O(2)–Ti(1)–C(29)	103.0 (1)	O(2)–Zr(1)–C(33)	103.1 (2)
O(2)–Ti(1)–C(30)	103.3 (1)	O(2)–Zr(1)–C(34)	106.3 (2)
O(15)–Ti(1)–O(28)	109.6 (1)	O(17)–Zr(1)–O(32)	106.7 (2)
O(15)–Ti(1)–N(31)	112.6 (1)	O(17)–Zr(1)–N(35)	109.2 (2)
O(15)–Ti(1)–C(29)	140.8 (1)	O(17)–Zr(1)–C(33)	134.2 (2)
O(15)–Ti(1)–C(30)	142.8 (1)	O(17)–Zr(1)–C(34)	135.3 (2)
O(28)–Ti(1)–N(31)	90.1 (1)	O(32)–Zr(1)–N(35)	84.2 (2)
O(28)–Ti(1)–C(29)	34.8 (1)	O(32)–Zr(1)–C(33)	32.5 (2)
O(28)–Ti(1)–C(30)	65.1 (1)	O(32)–Zr(1)–C(34)	60.0 (2)
N(S1)–Ti(1)–C(29)	65.9 (1)	N(35)–Zr(1)–C(33)	61.8 (3)
N(S1)–Ti(1)–C(30)	35.5 (1)	N(35)–Zr(1)–C(34)	33.7 (3)
Ti(1)–O(2)–C(3)	170.9 (3)	Zr(1)–O(2)–C(3)	170.1 (4)
Ti(1)–O(15)–C(16)	172.3 (3)	Zr(1)–O(17)–C(18)	170.4 (5)
Ti(1)–O(28)–C(29)	93.9 (2)	Zr(1)–O(32)–C(33)	96.1 (4)
Ti(1)–N(31)–C(30)	93.5 (2)	Zr(1)–N(35)–C(34)	94.4 (5)

Table II. Selected Bond Distances (Å) and Angles (deg) for IIc

Ti(1)–O(10)	1.845 (4)	Ti(1)–C(300)	2.399 (6)
Ti(1)–O(20)	1.790 (4)	N(100)–C(200)	1.397 (7)
Ti(1)–N(100)	1.919 (5)	C(200)–C(300)	1.405 (8)
Ti(1)–N(400)	1.844 (5)	C(300)–N(400)	1.392 (8)
Ti(1)–C(200)	2.408 (6)		
O(10)–Ti(1)–O(20)	110.3 (2)	N(100)–Ti–N(400)	89.0 (2)
O(10)–Ti(1)–N(100)	120.0 (2)	N(100)–Ti–C(200)	35.3 (2)
O(10)–Ti(1)–N(400)	116.1 (2)	N(100)–Ti–C(300)	66.1 (2)
O(10)–Ti(1)–C(200)	105.0 (2)	N(400)–Ti–C(200)	66.1 (2)
O(10)–Ti(1)–C(300)	103.3 (2)	N(100)–Ti–C(300)	35.4 (2)
O(20)–Ti(1)–N(100)	109.4 (2)	Ti(1)–O(10)–C(11)	154.5 (4)
O(20)–Ti(1)–N(400)	110.3 (2)	Ti(1)–O(20)–C(21)	173.9 (4)
O(20)–Ti(1)–C(200)	141.1 (2)	Ti(1)–N(100)–C(200)	91.9 (4)
O(20)–Ti(1)–C(300)	141.8 (2)	Ti(1)–N(400)–C(300)	92.9 (4)

oxygen atoms (vide infra). The most notable feature of the two structures is the distinct lack of planarity of the two 5-membered chelate rings. This bending results in the two carbon atoms of the chelate ring being brought toward the metal atom. This aspect of the coordination properties will be discussed at length below. However, the folding of the chelate results in the two aryloxide ligands becoming non-equivalent. In solution the ^1H and ^{13}C NMR spectra of Ia and Ib at ambient temperatures indicate the presence of only one type of aryloxide ligand. Furthermore the two non-equivalent benzyl ligands display two sharp singlets for their methylene protons. A static, nonplanar geometry would result in both of these groups becoming diastereotopic. Sharp NMR spectra are maintained in solution even down to −75 °C in toluene-d_8. Hence we conclude that the molecules either adopt a planar geometry in solution or, more likely based on the data for the enediamido complexes below, are very fluxional on the NMR time scale involving rapid flipping of the 5-membered metallacycle. Attempts to identify conclusively the resonances due to the carbon atoms in the chelate ring were unsuccessful. In the ^{13}C NMR spectra of I a large number of peaks between δ 115 and 165 are present. The use of a combination of routine ^1H coupling and APT techniques identified those carbons devoid of protons but still did not lead to a conclusive assignment.

Ti(OAr-2,6Pr$^i_2$)$_2$[xyNC(CH$_2$Ph)=C(CH$_2$Ph)NBu^t] (IIc) and Zr(OAr-2,6Bu$^t_2$)$_2$[xyNC(CH$_3$)=C(CH$_3$)Nxy] (IId). The molecular structures of IIc and IId are shown in Figures 3 and 4 while

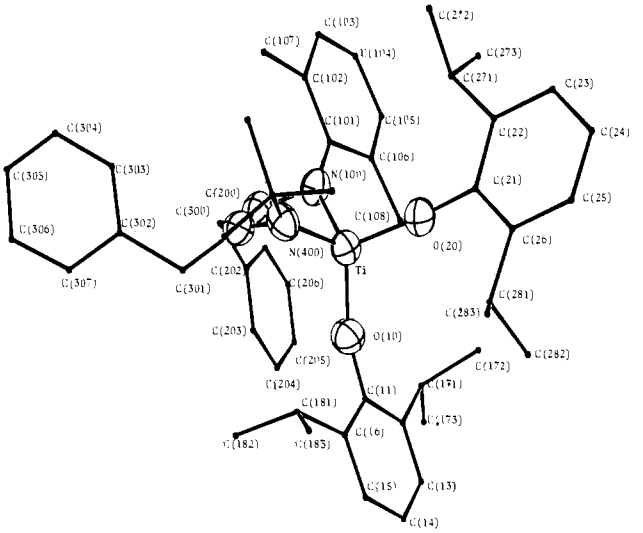

Figure 3. ORTEP view of Ti(OAr-2,6Pr$^i_2$)$_2$[xyNC(CH$_2$Ph)=C(CH$_2$Ph)NBu^t] (IIc).

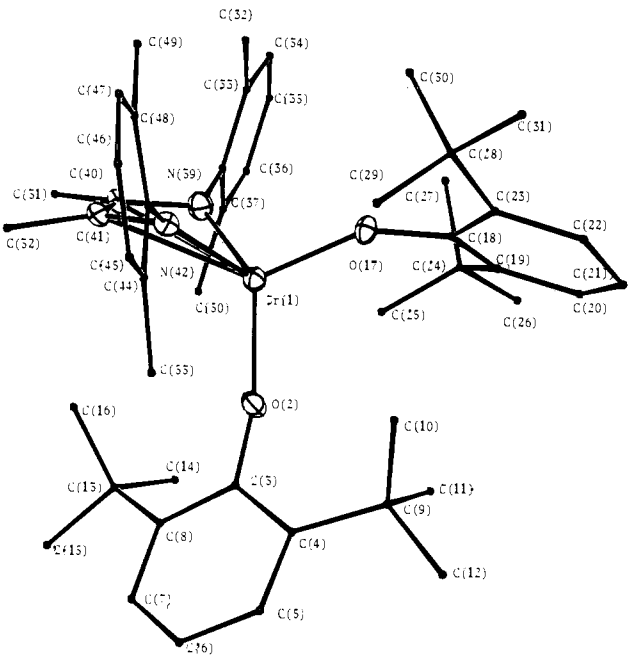

Figure 4. ORTEP view of Zr(OAr-2,6Bu$^t_2$)$_2$[xyNC(CH$_3$)=C(CH$_3$)Nxy] (IId).

Table III. Selected Bond Distances (Å) and Angles (deg) for IId

Zr(1)–O(2)	2.009 (4)	N(39)–C(40)	1.420 (8)
Zr(1)–O(17)	1.950 (4)	C(40)–C(41)	1.366 (9)
Zr(1)–N(39)	2.060 (6)	C(41)–N(42)	1.439 (8)
Zr(1)–N(42)	2.061 (15)		
Zr(1)–C(41)	2.698 (7)		
O(2)–Zr(1)–O(17)	114.0 (2)	N(39)–Zr(1)–N(42)	84.1 (2)
O(2)–Zr(1)–N(39)	125.8 (2)	N(39)–Zr(1)–C(41)	58.5 (2)
O(22)–Zr(1)–N(42)	114.2 (2)	N(42)–Zr(1)–C(41)	31.7 (2)
O(2)–Zr(1)–C(41)	111.9 (2)	Zr(1)–O(2)–C(3)	156.5 (4)
O(17)–Zr(1)–N(39)	105.3 (2)	Zr(1)–O(17)–C(18)	151.9 (4)
O(17)–Zr(1)–N(42)	109.3 (2)	Zr(1)–N(39)–C(40)	102.0 (4)
O(17)–Zr(1)–C(41)	130.6 (2)	Zr(1)–N(42)–C(41)	99.4 (4)

some selected bond distances and angles are collected in Tables II and III respectively for IIc and IId. Again a pseudotetrahedral coordination about the metal is obtained for both compounds with a nonplanar 5-membered chelate ring clearly related to the observed structure of Ia and Ib. The M(OAr)$_2$ fragments in Ia, Ib, IIc, and IId are almost identical. However, unlike their enamidolate counterparts, the ^1H NMR spectra of all of the ene-

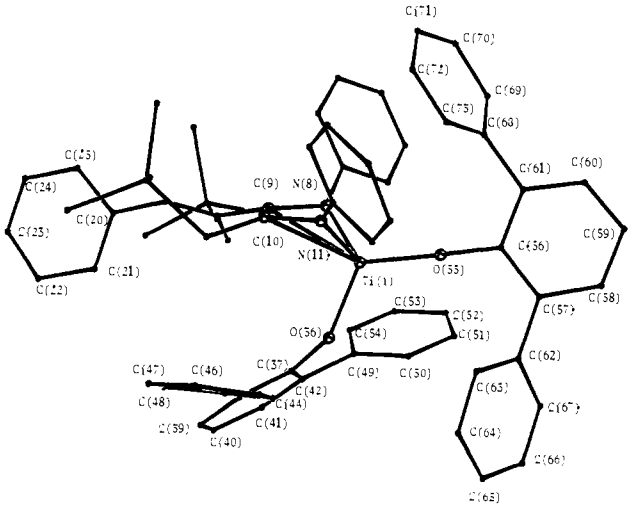

Figure 5. ORTEP view of $Ti(OAr\text{-}2,6Ph_2)_2[PhNCR{=}C(CR{=}NPh)NPh]$ (III) (R = CH_2SiMe_3).

Table IV. Selected Bond Distances (Å) and Angles (deg) for III

Ti(1)–O(36)	1.856 (7)	N(8)–C(9)	1.407 (12)
Ti(1)–O(55)	1.811 (7)	C(9)–C(10)	1.419 (13)
Ti(1)–N(8)	1.883 (9)	C(10)–N(11)	1.389 (12)
Ti(1)–N(11)	1.921 (8)	N(19)–C(18)	1.295 (13)
Ti(1)–C(9)	2.447 (10)		
Ti(1)–C(10)	2.478 (11)		
O(36)–Ti(1)–O(35)	117.8 (3)	Ti(1)–O(36)–C(37)	146.0 (7)
O(36)–Ti(1)–N(8)	113.5 (3)	Ti(1)–O(55)–C(56)	174.6 (7)
O(36)–Ti(1)–N(11)	112.2 (4)	Ti(1)–N(8)–C(9)	95.0 (6)
O(36)–Ti(1)–C(9)	96.8 (3)	Ti(1)–N(11)–C(10)	95.6 (6)
O(36)–Ti(1)–C(10)	96.1 (3)	N(8)–Ti(1)–N(11)	86.9 (4)
O(55)–Ti(1)–N(8)	112.3 (4)		
O(55)–Ti(1)–N(11)	110.0 (3)		
O(55)–Ti(1)–C(9)	143.0 (4)		
O(55)–Ti(1)–C(10)	141.1 (3)		

diamido complexes II are broad at ambient temperatures. On cooling the spectra broaden further before sharpening up. The final, limiting low-temperature spectra are totally consistent with the observed solid-state structures of IIc and IId. Specifically the nonplanar chelate ring results in the presence of two, nonequivalent sets of aryloxide signals in the ^1H NMR spectrum. Furthermore for the three benzyl derivatives IIa–IIc the methylene protons appear as AB quartets. The nonplanar chelate prohibits a plane of symmetry passing through these groups making the protons diastereotopic. For the 2,6-dimethylphenyl (xy) containing species, non-equivalent xylyl methyl groups are also observed at low temperature. This is indicative of restricted rotation about the xy–N bonds. On warming the nonequivalent signals broaden, coalescence, and finally give rise to a sharp spectrum. Hence at higher temperatures flipping of the chelate ring becomes rapid on the NMR time scale. Analysis of the spectra allows one to estimate the activation energy for ring flipping at the coalescence temperature, T_c. These data are discussed in more detail below. Again the conclusive identification of the N*C*–*C*N carbon resonance in the ^{13}C NMR spectra of II was not achieved. An interesting feature of the ^1H NMR spectra of the asymmetric enediamido complexes IIb and IIc is the presence of non-equivalent CH_3 resonances for the $CH(CH_3)_2$ groups of the aryloxide ligands even at high temperature. Irrespective of the rate of ring flipping, the asymmetric chelate results in these methyl groups within the equivalent Pr^i groups becoming diastereotopic. An identical situation was found for the enamidolate Ia.

$Ti(OAr\text{-}2,6Ph_2)_2[PhNC(CH_2SiMe_3){=}C(CCH_2SiMe_3NPh)NPh]$ (III). Figure 5 illustrates the molecular structure of III while Table IV contains some selected bond distances and angles. The molecular structure of III can be seen to be closely related to that found for IIc and IId. Again a nonplanar five-membered ring is present, bound to a $Ti(OAr)_2$ fragment (Figure 6). However,

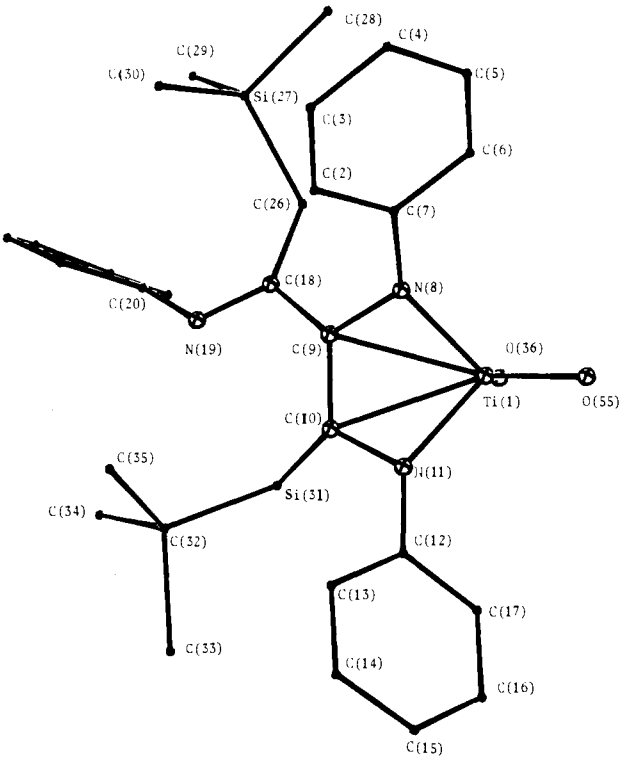

Figure 6. ORTEP view of III emphasizing the central coordination sphere.

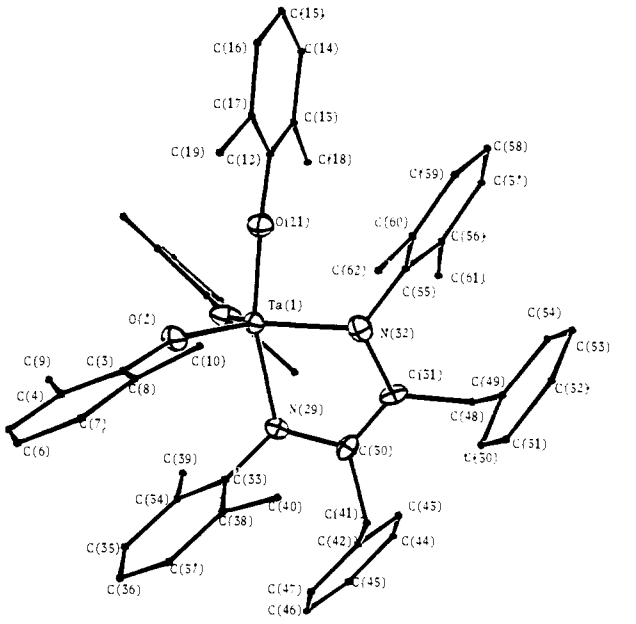

Figure 7. ORTEP view of $Ta(OAr\text{-}2,6Me_2)_3[xyNC(CH_2Ph){=}C(CH_2Ph)Nxy]$ (IV).

the backbone of the chelate ring in III contains an imino function (–CR=NAr) bound to one of the carbon atoms instead of a simple alkyl group as is present for complexes of type II. This appears to have little effect on the coordination properties of the enediamido chelate and furthermore the temperature dependence of the ^1H NMR spectra of III is similar to that found for II. At ambient temperatures the two non-equivalent CH_2SiMe_3 groups are clearly resolved. On cooling, the CH_2SiMe_3 methylene protons broaden and separate out into two AB patterns indicating the slowing down of the ring-flipping process.

$Ta(OAr\text{-}2,6Me_2)_3[xyNC(CH_2Ph){=}C(CH_2Ph)Nxy]$ (IV). The molecular structure of IV is shown in Figure 7. Table V contains the fractional coordinates and some selected bond distances and angles, respectively. The molecule can be seen to adopt a geometry about the metal best described as trigonal bipyramidal. The

Table V. Selected Bond Distances (Å) and Angles (deg) for IV

Ta(1)-O(2)	1.898 (5)	N(29)-C(30)	1.409 (11)
Ta(1)-O(11)	1.904 (6)	C(30)-C(31)	1.352 (11)
Ta(1)-O(20)	1.880 (6)	C(31)-N(32)	1.432 (10)
Ta(1)-N(29)	2.084 (7)		
Ta(1)-N(32)	2.041 (7)		
O(2)-Ta(1)-O(11)	95.4 (3)	N(29)-Ta(1)-N(32)	74.6 (3)
O(2)-Ta(1)-O(20)	109.7 (3)	Ta(1)-O(2)-C(3)	162.9 (5)
O(2)-Ta(1)-N(29)	90.9 (3)	Ta(1)-O(11)-C(12)	171.5 (6)
O(2)-Ta(1)-N(32)	135.8 (3)	Ta(1)-O(20)-C(21)	166.6 (5)
O(11)-Ta(1)-O(20)	97.1 (2)	Ta(1)-N(29)-C(30)	118.0 (5)
O(11)-Ta(1)-N(29)	161.2 (3)	Ta(1)-N(32)-C(31)	119.4 (5)
O(11)-Ta(1)-N(32)	88.7 (3)		

Scheme V

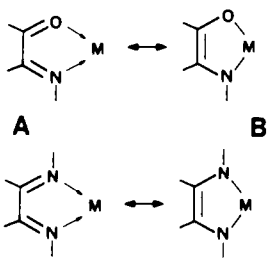

nitrogen atoms of the chelating enediamido ligand occupy one axial and one equatorial site. Presumably the 75° bite of the ligand is better accommodated this way than if both nitrogen atoms were equatorial. In contrast to the group 4 metal aryloxide derivatives discussed previously, the 5-membered metallacycle in IV is planar. Only one set of OAr-2,6Me_2 and xylyl methyl resonances is observed in the ^{1}H NMR spectrum of IV indicating that the molecule is fluxional on the NMR time scale in solution resulting in the aryloxide ligands as well as both ends of the chelate becoming equivalent.

Coordination Properties of the Enamidolate and Enediamido Ligands. The chelating ligands formed by the intramolecular coupling of η^2-acyl or η^2-iminoacyl functions can be assigned two resonance forms (Scheme V). In this respect they are related to a host of other bidentate chelates. This resonance variability has probably been most studied for transition-metal butadiene,[22] dithiolene,[23] and catecholate[24] complexes. For the ligands obtained in this study the two resonance forms are illustrated (Scheme V). In resonance A the chelate is considered to be a neutral organic fragment, i.e., either an α-ketoimine (1-oxa-4-aza-1,3-butadiene)[25] or α-diimine (1,4-diaza-1,3-butadiene)[26,27] molecule. In resonance B this fragment has been doubly reduced by the metal to produce enamidolate and enediamido groups, respectively. The formal oxidation state of the metal varies by two between the two forms. Specifically, for the group 4 and group 5 metals involved in this study the representations result in a d^2 and d^0 metal configuration for A and B, respectively.

The structural data we have obtained for our compounds are entirely consistent with the bonding picture represented by resonance B. Selected bond distances that hightlight this are grouped together in Table VI along with some structural data reported in the literature on an uncoordinated 1,4-diaza-1,3-butadiene ligand and one of its complexes.[26] It can be seen (Table VI) that the C–N and C–O distances for the chelate rings are significantly longer than expected for double bonds and are much closer to single bond distances. The C–O distances of 1.373 (4) and 1.377 (9) Å found in Ia and Ib, respectively, can be compared with 1.26 Å typical for carbonyl groups[28] and 1.36–1.38 Å typical for the corresponding distance in coordinated alkoxides.[29] The C–N distances vary from 1.389 (12) to 1.439 (8) Å in compounds I–IV, much longer than the 1.277 (?) Å reported for (dab)Mo(CO)$_4$.[26] These distances are much closer to the values accepted for single bonds between sp^2-hybrized carbon and nitrogen.[30] The metallacycle found in compound III is of relevance of this point as it contains, besides the enediamide backbone, an imine functionality uncoordinated to the metal. Hence this C–N distance of 1.295 (13) Å can be taken as representative of a double bond. Considering the C–C distances in the six metallacycles characterized here, they can be seen to fall in the range 1.35–1.40 Å, except for complex III where a slightly longer distance of 1.42 (1) Å is observed. The former distances are slightly longer than the C–C distance of 1.33 Å found in ethylene.[30] However, the much longer C–C distance in III may be due to the presence of the non-innocent imine substituent bonded to one of these carbon atoms. The distances obtained in this study compare well with the C=C distance of 1.398 (4) Å reported for the complex (*s-cis*-2,3-dimethylbutadiene)zirconocene where a metallocyclopentene resonance is adopted.[31]

The metal–oxygen and metal–nitrogen distances to the chelate rings are also supportive of the resonance picture B. Hence the Ti–N and Zr–N distances of 1.88–1.92 and 2.03–2.06 Å, respectively, are very close to values normally associated with simple dialkylamido groups bound to these metals[32] and are considerably shorter than "dative" bonds such as to pyridine ligands.[33] This is also the case for the Ta–N bonds in IV.

The other interesting feature of these derivatives is the lack of planarity of the 5-membered metallacycles in the group 4 metal compounds I–III, either as demonstrated by structural studies or also by observed NMR fluxional behavior. The lack of planarity of a large number of early transition metal 5-membered metallacycles has been characterized in the literature. However, the most extensive and well-studied series are those based on the group 4 metal metallocenes of general formula $Cp_2M[XC(R)=C(R)X]$ (M = Ti, Zr, Hf; X = CR_2,[34] O,[17a,35] S,Se,[36] Te[37]). The C–C backbone is sometimes part of a benzene ring. Although the compounds I–III do not have their direct Cp_2M counterparts, they are clearly related. Tables VI and VII list the fold angle (θ) observed for those compounds structurally characterized in this study as well as the value of $\Delta G^{\ddagger}$ for the ring-flipping process estimated from coalescence temperatures. We believe we can draw the following conclusions based on the data. For the enediamido compounds the inversion barrier falls in the sequence Ti > Zr > Hf; compare compounds IIa with IId and IIf with IIg. Studies by Erker on the metallocene derivatives of butadiene ligands have consistently shown a higher barrier to inversion of Zr than Hf.[22] Furthermore a comparison of the inversion barriers for IIe and IIf indicates that the substituents on the carbon backbone can be important. The product IIe formed with benzyl substituents inverts much faster than the corresponding compound IIf with methyl substituents. This effect may be steric or electronic in nature.

(22) Erker, K.; Kruger, C.; Muller, G. *Adv. Organomet. Chem.* **1985**, *24*, 1 and references therein.
(23) (a) Eisenberg, R. *Prog. Inorg. Chem.* **1970**, *12*, 295. (b) Coucovanis, D. *Prog. Inorg. Chem.* **1970**, *11*, 233.
(24) (a) Camano, C. J.; Raymond, K. N. *Acc. Chem. Res.* **1979**, *12*, 183. (b) Pierpont, C. G.; Buchanan, R. M. *Coord. Chem. Rev.* **1981**, *38*, 45.
(25) Van Vliet, M. P. R.; Van Koten, G.; Rottereel, M. A.; Schrap, M.; Vrieze, K.; Kojic-Prodic, B.; Spek, A. L.; Duisenberg, A. J. M. *Organometallics* **1986**, *5*, 1389 and references therein.
(26) Van Koten, G.; Vrieze, K. *Adv. Organomet. Chem.* **1982**, *21*, 153.
(27) Cotton, F. A.; Wilkinson, G. *Comprehensive Inorganic Chemistry*; 4th ed.; John Wiley and Sons: New York, 1980.
(28) *Chem. Soc. Spec. Publ.* **1965**, *18*, 520.
(29) Chisholm, M. H.; Rothwell, I. P. *Comprehensive Coordination Chemistry*; Pergamon: New York, 1987; Vol. 2, Chapter 15.3.
(30) *CRC Handbook of Chemistry and Physics*, 62nd ed.; CRC Press: Boca Raten, FL, 1981; p 176.
(31) Erker, G.; Engel, K.; Kruger, C.; Muller, G. *Organometallics* **1984**, *3*, 128.
(32) Lappert, M. F.; Sanger, A. R.; Srivastava, R. C.; Power, P. P. *Metal and Metalloid Amides*; Horwood-Wiley: New York, 1979.
(33) (a) Moore, K. J.; Straus, D. a.; Armantrout, J.; Santarsiero, B. D.; Grubbs, R. H.; Bercaw, J. E. *J. Am. Chem. Soc.* **1983**, *105*, 2068. (b) Latesky, S. L.; McMullen, A. K.; Rothwell, I. P.; Huffman, J. C. *J. Am. Chem. Soc.* **1985**, *107*, 5981.
(34) Bristow, G. S.; Lappert, M. F.; Martin, T. R.; Atwood, J. L.; Hunter, W. F. *J. Chem. Soc., Dalton Trans.* **1984**, 399.
(35) Andra, K. *J. Organomet. Chem.* **1968**, *11*, 567.
(36) (a) Kopf, H.; Schmidt, M. *J. Organomet. Chem.* **1965**, *4*, 426. (b) Kopf, H.; Klapotke, T. *Z. Naturforsch.* **1986**, *41*, 667. (c) Kopf, H. *Angew. Chem.* **1971**, *83*, 146. (d) Kutoglv, A. *Z. Anorg. Allg. Chem.* **1972**, *390*, 195.
(37) Kopf, H.; Klapotke, T. *J. Chem. Soc., Chem. Commun.* **1986**, 1192.

Table VI. Selected Structural Data on Enamidolate and Enediamide Derivatives and Related Compounds

compd	M–N	M–O	N–C	O–C	C–C	M–C	θ, deg	ref
Ia	1.893 (3)	1.877 (3)	1.412 (5)	1.373 (4)	1.375 (6)	2.398 (4)	51.1	*a*
Ib	2.038 (6)	2.004 (5)	1.43 (1)	1.377 (9)	1.35 (1)	2.549 (8)	50.0	*a*
						2.581 (8)		
IIc	1.919 (5)		1.397 (7)		1.405 (8)	2.408 (6)	54.7	*a*
	1.844 (5)		1.392 (8)		2.399 (6)			
IId	2.060 (6)		1.420 (8)		1.366 (9)	2.698 (7)	37.8	*a*
	2.061 (15)		1.439 (8)					
III	1.883 (9)		1.41 (1)		1.42 (1)	2.45 (1)	53.9	
	1.921 (8)		1.39 (1)			2.48 (1)		
IV	2.084 (7)		1.41 (1)		1.35 (1)		0	*a*
	2.041 (7)		1.43 (1)					
$Cp^*_2Zr(OCMe{=}CMeO)$		2.031 (4)		1.371 (10)	1.315 (13)		16.8	17a
$C_6H_{11}N{=}CHCH{=}NC_6H_{11}$			1.257 (2)		1.457 (2)			26

Table VII. Estimated Barriers for the Ring Inversion of Enediamido Complexes

	$M(OAr)_2[R'NC(R){=}C(R)NR'']$					
	M	OAr	R	R′	R″	$\Delta G^{\ddagger}(T_c)^a$
IIa	Ti	OAr-2,6Pr^i_2	CH_2Ph	xy	xy	15.1 (40)
IIb	Ti	OAr-2,6Pr^i_2	CH_2Ph	Ph	Bu^t	15.6 (17)
IIc	Ti	OAr-2,6Pr^i_2	CH_2Ph	xy	Bu^t	17.1 (60)
IId	Zr	OAr-2,6Bu^t_2	CH_3	xy	xy	14.5 (0)
IIe	Zr	OAr-2,6Bu^t_2	CH_2Ph	Ph	Ph	12.7 (−15)
IIf	Zr	OAr-2,6Bu^t_2	CH_3	Ph	Ph	15.5 (35)
IIg	Hf	OAr-2,6Bu^t_2	CH_3	Ph	Ph	14.2 (10)

[a] ΔG° in kcal mol^{-1}; T_c in °C.

Erker has shown that 2,3-dimethylbutadiene inverts faster than simple, unsubstituted butadiene when bound to zirconocene.[31] Although there is a definite variation of the rate of ring flipping with nitrogen substituents, the dependency is not totally consistent. Hence on going from IId to IIf one finds an increase in the barrier, i.e., replacing N–Ph by N–xy; but a similar change on going from IIc to IIb has the opposite effect. The enamidolate complexes I both show large fold angles of approximately 50° in the solid state. However, even though this folding is much larger than that seen for the enediamide IId, these complexes both undergo much more rapid inversion as evidenced by the lack of freezing out of the inversion process even at −75 °C. The series of *o*-xylidene complexes $Cp_2M(CH_2C_6H_4CH_2)$ (M = Ti, Zr, Hf) studied by Lappert et al.[34] were also found to have fold angles of 50–53° in the solid state, although freezing out of the inversion process on the NMR time scale was not achieved. Kopf and co-workers have managed to synthesize and study the series of complexes $Cp_2Ti(XC_6H_4X)$ (X = S, Se, Te).[36,37] The inversion of the nonplanar metallacycles was monitored by using the non-equivalent Cp rings, and surprisingly the barrier was found to be relatively insensitive to the nature of X.

Another important consequence of the folding of these 5-membered metallacycles is the close approach thus achieved between the metal atom and the two carbon atoms of the chelate ring. This raises the question as to whether the bending of the chelate ring is caused by the electron deficient metal center trying to undergo π-bonding with the olefinic portion of the heteroatom-substituted metallocyclopentene backbone. This would lead to a description of the bonding as σ^2,π which can be represented as shown (Scheme VI). The metal–carbon distances relevant to this discussion are given in Table VI. For titanium the distances vary from 2.398 (4) Å in Ia to 2.48 (1) Å in III. These can be compared with normal Ti–C(alkyl) distances of 2.051 (4) Å in $Ti(OA\text{-}2,6Ph_2)_3(CH_2SiMe_3)$[38] and 2.095 (6) Å and 2.131 (6) Å in the monocyclometalated complex $Ti(OC_6H_3Bu^tCMe_2CH_2)(OAr\text{-}2,6Bu^t_2)(CH_2SiMe_3)(py)$.[33b] However, although much larger than these distances, the contacts seen in these complexes are comparable to the values 2.35–2.45 Å, found for the Ti–C(Cp) bond in cyclopentadiene complexes.[39] Similarly for the zirconium

Scheme VI

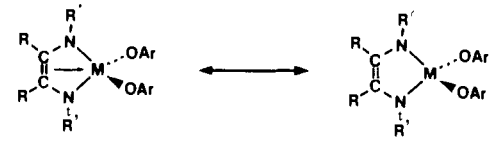

compounds Ib and IId the Zr–C distances of 2.55–2.27 Å are well beyond Zr–C (alkyl) bond lengths but again not too far outside the typical Zr–C(Cp) distances of 2.5 Å found in zirconocene derivatives.[39] Theoretical studies with the EHMO method have been carried out on the model compound $(MeO)_2Zr[MeNC(Me)C(Me)NMe]$ by Tatsumi et al.[40] The metallacycle was found to have a clear tendency to bend with a minimum energy lying at a fold angle of 40–45°. A Zr–C overlap population of 0.08–0.11 was found, indicating an attractive interaction between the metal and the N*C*=*C*N unit. Theoretical studies have also been reported on the enediolate complex $Cp_2Zr(OCR{=}CRO)$, and again a nonplanar metallacycle was predicted.[17a] Recent work by Curtis et al. on a structurally characterized, nonplanar metallacyclopentatriene ring bound to tantalum(V) indicated that the bending of the chelate was in order to relieve antibonding interactions present in a planar ring.[17b] The significant bending of the metallacycles bound to the group 4 metal $M(OAr)_2$ fragments contrasts with the almost perfectly planar geometry seen in complex IV. Presumably this reflects the differing electronic nature of the $Ta(OAr)_3$ fragment although theoretical studies of this molecule have yet to be undertaken.

Experimental Section

All operations were carried out under a dry nitrogen atmosphere either in a Vacuum Atmosphere dri-lab or by standard Schlenck techniques. The η^2-iminoacyl compounds were synthesized by previously reported methods,[15] except $Ti(OAr\text{-}2,6Pr^i_2)_2(\eta^2\text{-}xyNCCH_2Ph)(\eta^2\text{-}Bu^tNCCH_2Ph)$ and $Ti(OAr\text{-}2,6Pr^i_2)_2(\eta^2\text{-}PhNCCH_2Ph)(\eta^2\text{-}Bu^tNCCH_2Ph)$ (vide infra). ^1H and ^{13}C NMR spectra were recorded either on a Varian Associates XL-200 or Nicolet Instruments 470 MHz instrument. Reactions requiring pressure were carried out in a Parr minireactor. Because of the similarity of the procedures, only representative specific syntheses will be outlined in full.

Synthesis of Enamidolate Compounds (I). **$Ti(OAr\text{-}2,6Pr^i_2)_2[OC(CH_2Ph){=}C(CH_2Ph)NBu^t]$ (Ia).** A solution of $Ti(OAr\text{-}2,6Pr^i_2)_2(\eta^2\text{-}Bu^tNCCH_2Ph)(CH_2Ph)$ (typically 0.2–0.5 g) in benzene (20–50 cm^3) was loaded in a glass liner into a 300-cm^3 capacity Parr minireactor. After being pressurized with CO (1000 psi) for 24 h the bomb was vented and the resulting deep-red solution evaporated to give an essentially quantitative yield of the product as a dark-red solid. Crystals suitable for X-ray diffraction study could be readily grown from saturated hexane solutions on slow cooling. Anal. Calcd for $TiC_{44}H_{57}NO_3$: C, 75.95; H, 8.26; N, 2.01. Found: C, 75.82; H, 8.15; N, 2.13. ^1H NMR (C_6D_6, 30 C): δ 4.05 (s, $OCCH_2Ph$), 3.91 (s, Bu^tNCCH_2Ph), 1.21 (s, Bu^tN), 3.6 (septet, $CHMe_2$), 1.3 (m, $CHMe_2$).

$Zr(OAr\text{-}2,6Bu^t_2)_2[OC(CH_2Ph){=}C(CH_2Ph)Nxy]$ (Ib). This complex was synthesized with use of identical methods from $Zr(OAr\text{-}2,6Bu^t_2)_2(\eta^2\text{-}xyNCCH_2Ph)(CH_2Ph)$ and obtained as colorless blocks from hexane solvent. Anal. Calcd for $ZrC_{54}H_{65}NO_3$: C, 74.06; H, 7.77; N, 1.66. Found: C, 73.92; H, 8.01; N, 1.58. ^1H NMR (C_6D_6, 30 °C): δ 3.99

(38) Durfee, L.; Rothwell, I. P., results to be submitted for publication.
(39) *Comprehensive Organometallic Chemistry*; Abel, E., Stone, F. G. A., Wilkinson, G., Eds.; Pergamon: New York, 19??.
(40) Tatsumi, K., personal communication.

Table VIII. Crystal Structure Determination Data

	Ia	Ib		Ia	Ib
formula	$TiC_{44}H_{57}NO_3$	$ZrC_{54}H_{65}NO_3$	linear abs coeff, cm^{-1}	2.488	2.601
fw	695.84	851.33	temp, °C	−154	−160
space group	$P2_1/a$	$P\bar{1}$	detector aperture	3.0 mm wide × 4.0 mm high	
a, Å	19.877 (8)	20.445 (9)	takeoff angle, deg	2.0	2.0
b, Å	12.065 (4)	11.750 (4)	scan speed, deg/min	4.0	4.0
c, Å	16.939 (7)	10.059 (3)	scan width, deg	1.8 + dispersion	2.0 + dispersion
α, deg		93.63 (1)	bkgd counts, s	8	6
β, deg	102.79 (2)	88.56 (1)	2θ range, deg	6–45	6–45
γ, deg		88.73 (1)	unique data	5185	6318
Z	4	2	unique data width	3923	5100
V, Å^3	3961.49	2410.29	$F_o > 3.00\sigma(F)$		
density (calcd), g/cm^3	1.167	1.173	$R(F)$	0.0545	0.0802
crystal size, mm	0.36 × 0.28 × 0.25	0.18 × 0.18 × 0.22	$Rw(F)$	0.0528	0.0799
crystal color	red	colorless	goodness of fit	1.056	1.23
radiation	Mo Kα (λ = 0.71069 Å)		largest Δ/σ 0.05	0.05	0.05

	IIc	IId		IIc	IId
formula	$TiC_{52}H_{66}N_2O_2$	$ZrC_{48}H_{66}N_2O_2$	temp, °C	+22	−161
fw	799.02	794.28	detector aperture	(1.5 + tan θ) mm wide × 4.0 mm high	3.0 mm wide × 4.0 mm high
space group	$P2_1/c$	$P2_1/n$			
a, Å1	11.751 (4)	11.653 (6)	takeoff angle, deg.	–	2.0
b, Å	15.113 (4)	14.820 (2)	scan speed, deg/min	4.90	4.0
c, Å	26.282 (6)	16.510 (3)	scan width, deg	0.8 + 0.35 tan θ	2.0 + dispersion
α, deg			bkgd counts, s	50% of scan time	8
β, deg	92.13 (2)	95.60 (5)	2θ range, deg	4–45	6–45
γ, deg			unique data	6380	5594
Z	4	4	unique data width	2650	3729
V, Å^3	4664.0	4291.0	$F_o > 3.00\sigma(F)$		
density (calcd), g/cm^3	1.138	1.230	$R(F)$	0.058	0.0630
crystal size, mm	0.56 × 0.43 × 0.30	0.23 × 0.26 × 0.26	$Rw(F)$	0.079	0.0560
crystal color	orange	orange	goodness of fit	1.524	1.021
radiation	Mo Kα (λ = 0.71069 Å)		largest Δ/σ	0.06	0.05
linear abs coeff, cm^{-1}	2.18	2.88			

	III	IV		III	IV
formula	$TiSi_2C_{65}H_{63}N_3O_2 \cdot {}^1/_2C_6H_{14}$	$TaC_{56}H_{59}N_2O_3$	temp, °C	−155	−152
fw	1065.39	989.04	detector aperture	(1.5 + tan θ) mm wide × 4.0 mm high	3.0 mm wide × 4.0 mm high
space group	$P2_1/a$	$P2_1/c$			
a, Å	30.390 (15)	18.869 (8)	takeoff angle, deg.	?	2.0
b, Å	13.335 (6)	13.006 (4)	scan speed, deg/min	4.90	4.0
c, Å	15.232 (7)	21.971 (9)	scan width, deg	1.4 + dispersion	2.0 + dispersion
α, deg			bkgd counts, s	8	6
β, deg	105.04 (2)	119.46 (6)	2θ range, deg	6–45	6–45
γ, deg			unique data	7850	6121
Z	4	4	unique data width		
V, Å^3	5969.98	4694.60	$F_o > 3.00\sigma(F)$	2878	4976
density (calcd), g/cm^3	1.185	1.399	$R(F)$	0.0718	0.0478
crystal size, mm	0.25 × 0.30 × 0.35	0.14 × 0.14 × 0.19	$Rw(F)$	0.0659	0.0454
crystal color	red	red	goodness of fit	1.037	1.003
radiation	Mo Kα (λ = 0.71069 Å)		largest Δ/σ	0.10	0.05
linear abs coeff, cm^{-1}	2.24	23.57			

(s, $OCCH_2Ph$), 3.51 (s, xyNCCH_2Ph), 1.40 (s, Bu^t), 1.93 (s, xy-*Me*).

Synthesis of Enediamido Compounds (II). Ti(OAr-2,6Pr$^i_2$)$_2$[xyNC(CH$_2$Ph)=C(CH$_2$Ph)Nxy] (IIa). Thermolysis of Ti(OAr-2,6Pr$^i_2$)$_2$(η^2-xyNCCH$_2$Ph)$_2$ in toluene at 117 °C for 2 h resulted in the formation of a deep-red solution of the coupled product. Removing the solvent under vacuum, dissolving the residue in warm hexane, and cooling the solution to −15 °C gave the product as orange crystals. Anal. Calcd for $TiC_{56}H_{66}N_2O_2$: C, 79.39; H, 7.87; N, 3.31. Found: C, 78.55; H, 7.79; N, 3.18. ^{1}H NMR ($C_6D_5CD_3$, −10 °C): δ 4.35 (d), 3.60 (d, CCH_2Ph), 2.21 (s), 1.78 (s, xy-CH_3), 3.50 (br, CHMe$_2$), 0.8–1.4 (series of overlapping doublets, CHMe_2).

Ti(OAr-2,6Pr$^i_2$)$_2$[PhNC(CH$_2$Ph)=C(CH$_2$Ph)NBu^t] (IIb). The addition of PhNC (1 equiv) to hydrocarbon solutions of Ti(OAr-2,6Pr$^i_2$)$_2$(η^2-Bu^{t}NCCH$_2$Ph)(CH$_2$Ph) results in the initial formation of Ti(OAr-2,6Pr$^i_2$)$_2$(η^2-Bu^{t}NCCH$_2$Ph)(η^2-PhNCCH$_2$Ph): ^{1}H NMR (C_6D_6, 30 °C): δ 3.68 (s), 4.05 (s, CCH_2Ph), 1.28 (s, NBu^t), 3.25 (septet, CHMe$_2$), 1.06 (d), 1.12 (d, CHMe_2). On standing for 2 h, intramolecular coupling to generate IIB occurred. Anal. Calcd for $TiC_{50}H_{62}N_2O_2$: C, 77.89; H, 8.11; N, 3.63. Found: C, 76.48; H, 8.04; N, 3.90. ^{1}H NMR ($C_6D_5CD_3$, 30 °C): δ 3.84 (d), 4.06 (d), 3.97 (d), 4.43 (d), CCH_2Ph), 1.24 (s, NBu^t), 3.40 (septet), 3.61 (septet, CHMe$_2$), 1.01 (d), 1.05 (d), 1.17 (d), 1.20 (d, CHMe_2). ^{13}C NMR (C_6D_6, 30 °C): δ 23.5, 23.7, 23.8, 24.1 (CHMe_2), 26.9, 27.1 (CHMe$_2$), 32.2 (NCMe_3), 34.7, 36.3 (C CH_2Ph), 61.1 (NCMe$_3$).

Ti(OAr-2,6Pr$^i_2$)$_2$[xyNC(CH$_2$Ph)=C(CH$_2$Ph)NBu^t] (IIc). A similar procedure to that used for IIb except with xyNC (1 equiv) allowed the isolation of stable Ti(OAr-2,6Pr$^i_2$)$_2$(η^2Bu^{t}NCCH$_2$Ph)(η^2-xyNCCH$_2$Ph) as a yellow orange solid. Anal. Calcd for $TiC_{52}H_{66}N_2O_2$: C, 78.17; H, 8.33; N, 3.51. Found: C, 74.25; H, 7.72; N, 3.31. ^{1}H NMR (C_6D_6, 30 °C): δ 3.47 (s), 4.03 (s, CCH_2Ph), 1.15 (s, NBu^t), 1.69 (s, xy-Me), 1.18 (d), 1.11 (d, CHMe_2), 3.30 (septet, CHMe$_2$). ^{13}C NMR (C_6D_6, 30 °C): δ 232.2, 255.2, (η^2-CN). Thermolysis of this product at 100 °C for 4 h gave the coupled product IIc as orange crystals from hexane. ^{1}H NMR (C_6D_6, °C): δ 3.97 (d), 4.62 (d), 3.31 (d), 3.92 (d, CH_2Ph), 1.25 (s, NBu^t), 1.93 (s), 2.13 (s, xy-CH_3), 3.4–3.5 (br, CHMe$_2$), 0.96–1.3 (doublets, CHMe_2).

The coupled products IId–IIg were obtained on thermolysis of the corresponding bis η^2-iminoacyl in toluene at 100 °C.

Zr(OAr-2,6Bu$^t_2$)$_2$[xyNC(CH$_3$)=C(CH$_3$)Nxy] (IId): ^{1}H NMR ($C_6D_5CD_3$, −20 °C) δ 1.70 (s, NCCH_3), 2.15 (s), 2.32 (s, xyCH_3), 1.16 (s), 1.34 (s, Bu^t). Anal. Calcd for $ZrC_{48}H_{66}N_2O_2$: C, 72.59; H, 8.38; N, 3.63. Found: C, 72.38; H, 8.37; N, 3.19.

Zr(OAr-2,6Bu$^t_2$)$_2$[PhNC(CH$_2$Ph)=C(CH$_2$Ph)NPh] (IIe): ^{1}H NMR ($C_6D_5CD_3$, −20 °C) δ 3.41 (d), 4.12 (d, CH_2Ph), 1.19 (s), 1.69 (s, Bu^t).

Zr(OAr-2,6Bu$^t_2$)$_2$[PhNC(CH$_3$)=C(CH$_3$)NPh] (IIf): ^{1}H NMR ($C_6D_5CD_3$, 20 °C) δ 2.09 (s, NCCH_3), 1.55 (s, Bu^t). Anal. Calcd for $ZrC_{44}H_{58}N_2O_2$: C, 71.59; H, 7.92; N, 3.79. Found: C, 71.27; H, 8.22; N, 3.94.

Hf(OAr-2,6Bu$^t_2$)$_2$[PhNC(CH$_3$)=C(CH$_3$)NPh] (IIg): ^{1}H NMR ($C_6D_5CD_3$, −20 °C) δ (s, NCCH_3), (s), (s, Bu^t). Anal. Calcd for $HfC_{44}H_{58}N_2O_2$: C, 64.02; H, 7.08; N, 3.39. Found: C, 64.20; H, 7.37; N, 3.20.

Synthesis of $Ti(OAr\text{-}2,6Ph_2)_2[PhNC(CH_2SiMe_3)=C(CCH_2SiMe_3NPh)NPh]$ (III). A yellow solution of $Ti(OAr\text{-}2,6Ph)_2(\eta^2\text{-}PhNCCH_2SiMe_3)(CH_2SiMe_3)$ (0.5 g) in hexane (20 cm^3) was treated with 2 equiv of PhNC. After 6 h, the red supernatant solution was decanted from a few yellow crystals of starting material and allowed to stand, whereupon dark red crystals of $Ti(OAr\text{-}2,6Ph_2)_2[PhNC(CH_2SiMe_3)=C(CCH_2SiMe_3NPh)NPh]$ began to form and were finally isolated after a few hours. Cooling of the supernatant solution resulted in the formation of more red crystalline product.

Anal. Calcd for $TiC_{65}H_{63}N_3O_2Si_2\cdot{}^1/_2C_6H_{14}$: C, 76.66; H, 6.62; N, 3.94. Found: C, 76.29; H, 6.65; N, 3.66. ^1H NMR ($C_6D_5CD_3$, 30 °C): δ -0.73 (s), -0.01 (s, CH_2SiMe_3), 1.30 (d), 2.54 (d, CH_2SiMe_3), 5.68 (d), 6.5-7.1 (m, aromatics), 0.84 (m), 1.18 (m, hexane).

Synthesis of $Ta(OAr\text{-}2,6Me_2)_3[xyNC(CH_2Ph)=C(CH_2Ph)Nxy]$ (IV). Thermolysis of $Ta(OAr\text{-}2,6Me_2)_3(\eta^2\text{-}xyNCCH_2Ph)_2$ in toluene at 110 °C for 48 h produced the crude product as a yellow oil on removal of solvent. On allowing the oil to stand in contact with hexane, amber crystals of the product suitable for X-ray diffraction studies were obtained. ^1H NMR (C_6D_6, 30 °C): δ 1.95 (s, OAr-CH_3), 1.96 (s, Nxy-CH_3), 4.07 (s, NCCH_2Ph).

Crystallographic Studies. Five of the six structure determinations were obtained through the Molecular Structure Center of Indiana University[41] while the sixth, that of IIg, was done in house.[42] Crystal parameters are given in Table VIII. In all structures except III all non-hydrogen atoms were refined anisotropically. For compounds Ia, IId, and IV the hydrogen atoms were located and refined isotropically while for IIb and IIc they were placed in idealized positions. Further details of the crystallographic studies are contained in the supplementary material.

Acknowledgment. We thank the Department of Energy (Pittsburgh Energy Technology Center; Grant DE-Fg 22-85PC80909) and the National Science Foundation (Grant CHE-8612063) for support of this research. I.P.R. gratefully acknowledges the Camille and Dreyfus Foundation for the award of a Teacher Scholar Grant as well as the Alfred P. Sloan Foundation for the award of a Fellowship.

Supplementary Material Available: Tables of fractional coordinates and isotropic thermal parameters and complete bond distances and angles for Ia, Ib, IIc, IId, III, and IV (80 pages); tables of observed and calculated structure factors (68 pages). Ordering information is given on any current masthead page.

(41) Huffman, J. C.; Lewis, L. N.; Caulton, K. G. *Inorg. Chem.* **1980**, *19*, 2755.

(42) Fanwick, P. E.; Ogilvy, A. E.; Rothwell, I. P. *Organometallics* **1987**, *6*, 73.

Hydrogen Atom Abstraction from C-H, P-H, Si-H, and Sn-H Bonds by the Triplet Excited State of the Tetrakis(μ-pyrophosphito)diplatinum(II) Tetraanion. Spectroscopic Observation of the Mixed-Valence Hydride Complex $Pt_2(\mu\text{-}P_2O_5H_2)_4H^{4-}$

D. Max Roundhill,*[1a] Stephen J. Atherton,[1b] and Zhong-Ping Shen[1a]

Contribution from the Department of Chemistry, Tulane University, New Orleans, Louisiana 70118, and Center for Fast Kinetics Research, University of Texas at Austin, Austin, Texas 78712. *Received February 6, 1987*

Abstract: Pulse radiolysis of aqueous solutions of $Pt_2(\mu\text{-}P_2O_5H_2)_4^{4-}$ at pH 4 with added *t*-BuOH gives $Pt_2(\mu\text{-}P_2O_5H_2)_4H^{4-}$ via reaction with an electron and a proton. Pulsed-laser photolysis (Nd-YAG at 355 nm) of aqueous solutions of $Pt_2(\mu\text{-}P_2O_5H_2)_4^{4-}$ with added isopropyl alcohol, phosphorous acid, or hypophosphorous acid also gives $Pt_2(\mu\text{-}P_2O_5H_2)_4H^{4-}$ by hydrogen atom abstraction. The mixed-valence hydride is similarly formed in methanolic solutions of $(PPN)_4[Pt_2(\mu\text{-}P_2O_5H_2)_4]$ from added triethylsilane or tributyltin hydride. The intermediacy of the $Me_2\dot{C}OH$ radical is evidenced by the formation of both pinacol and acetone in the photochemically catalyzed dehydrogenation of isopropyl alcohol with $Pt_2(\mu\text{-}P_2O_5H_2)_4^{4-}$ in aqueous solution. The other radical, $Pt_2(\mu\text{-}P_2O_5H_2)_4H^{4-}$, disproportionates to $Pt_2(\mu\text{-}P_2O_5H_2)_4H_2^{4-}$ and $Pt_2(\mu\text{-}P_2O_5H_2)_4^{4-}$. The $Bu_3\dot{S}n$ radical has been detected by transient difference laser spectroscopy in solutions containing $Pt_2(\mu\text{-}P_2O_5H_2)_4^{4-}$ and Bu_3SnH. The quenching rates for hydrogen atom donors with the $^3A_{2u}$ state of $Pt_2(\mu\text{-}P_2O_5H_2)_4^{4-*}$, as measured by the Stern-Volmer equation, are given and compared.

The tetrakis(μ-pyrophosphito)diplatinum(II) tetraanion continues to be increasingly studied because of reports of the high chemical reactivity of its long-lived triplet ($^3A_{2u}$) excited state $Pt_2(\mu\text{-}P_2O_5H_2)_4^{4-*}$. A recent example that has generated interest is the discovery that the complex is a catalyst for the photochemical conversion of isopropyl alcohol into hydrogen and acetone.[2] A second catalytic application is the use of the complex in the photochemically induced hydrogen atom transfer from isopropyl alcohol to cyclohexene to give acetone and cyclohexane.[3] In each case it was suggested that the reaction pathway involved hydrogen atom transfer from isopropyl alcohol to the $^3A_{2u}$ state of $Pt_2(\mu\text{-}P_2O_5H_2)_4^{4-*}$, but no supportive evidence was offered in either case. We have now for the first time detected the mixed-valence $Pt^{II}Pt^{III}$ complex $Pt_2(\mu\text{-}P_2O_5H_2)_4H^{4-}$ in aqueous solutions and have found that the compound is also formed by direct hydrogen atom abstraction from the methine group of isopropyl alcohol.

Although the 1- and 2-electron oxidation of $Pt_2(\mu\text{-}P_2O_5H_2)_4^{4-}$ is well documented and now relatively well understood,[4] there has been minimal research on the reduction of this Pt^{II}_2 complex. Two such reports are the 1-electron reduction to $Pt_2(\mu\text{-}P_2O_5H_2)_4^{5-}$ and

(1) (a) Tulane University. (b) University of Texas at Austin.
(2) Roundhill, D. M. *J. Am. Chem. Soc.* **1985**, *107*, 4354-4356.
(3) Che, C.-M.; Lee, W.-M. *J. Chem. Soc., Chem. Commun.* **1986**, 512-513.
(4) Bryan, S. A.; Dickson, M. K.; Roundhill, D. M. *J. Am. Chem. Soc.* **1984**, *106*, 1882-1883. Bryan, S. A.; Schmehl, R. H.; Roundhill, D. M. *J. Am. Chem. Soc.* **1986**, *108*, 5408-5412. Roundhill, D. M.; Atherton, S. J. *J. Am. Chem. Soc.* **1986**, *108*, 6829-6831.

0002-7863/87/1509-6076$01.50/0